CHAPTER 11

METHOD OF ANALYSIS OF RANDOM WAVE EXPERIMENTS WITH REFLECTING COASTAL STRUCTURES

by

Pierre Gaillard, Michel Gauthier and Forrest Holly
Sogreah, Grenoble, France

ABSTRACT

A method of evaluation of the incident and reflected wave spectra in laboratory experiments or field investigations, based on the analysis of wave records obtained with a three-gauge array, is presented.

Results of a laboratory investigation with a rubble-mound breakwater and with a special type of sea-wall (ARC system) are given to illustrate the applications of the method.

INTRODUCTION

Random wave experiments performed with reflecting coastal structures require calibration of the wave generator movement in order to obtain incident waves conforming to specified characteristics. This calibration raises a problem because of multiple wave reflections from the structure and the wave paddle.

A technique often used in such cases, as well as in field investigations, consists in measuring the water level variation in front of the structure and in applying a method of analysis which estimates the incident and reflected waves.

Several methods of analysis based on measurements with two wave-gauges have formerly been published by Kajima [3], Thornton and Calhoun [5], Goda and Suzuki [2], Morden, Richey and Christensen [4]. In these methods, however, the incident wave spectral density cannot be estimated correctly in the vicinity of a discrete number of critical frequencies, for which the distance between the two wave-gauges is a multiple of half the corresponding wave-length.

In this paper a different method, based on the analysis of wave records obtained with a three gauge array is presented. With this method, it is possible to estimate the incident and reflected wave spectra for the whole range of frequencies of interest.

BASIC ASSUMPTIONS

The incident waves are considered as a stationary, ergodic random process with gaussian properties. The water surface level variations related to waves propagating along the positive x axis are accordingly represented by:

$$\eta_I(x,t) = \mathrm{Re}\ \{\ 2\int_0^\infty e^{i(2\pi ft - mx + \phi)}\ \sqrt{S_I(f)df}\} \tag{1}$$

with:

$$4\pi^2 f^2 = mg\ \tanh\ (mh) \tag{2}$$

f = wave frequency
m = wave number
h = Water depth at rest
ϕ = random phase with constant probability density
S_I = two-sided power spectral density of the incident waves

We shall consider a coastal structure in the wave tank, with its longitudinal axis parallel to the wave fronts. The structure section is assumed uniform so that diffraction effects are negligible. The reflected waves can thus be represented by:

$$\eta_r(x,t) = \mathrm{Re}\ \{\ 2\int_0^\infty T(x,f)\ e^{i(2\pi ft - mx + \phi)}\ \sqrt{S_I(f)df}\ \} \tag{3}$$

The transfer function $T(x,f)$ related to the wave reflection, is a function of the location of the point of observation, and of frequency. In the following, we consider as reference the abscissa x_s of the seaward face of the structure, where the transfer function takes the value:

$$T_s = T(x_s,f) = C_R(f)\ e^{i\phi_s(f)} \tag{4}$$

$C_R(f)$: reflection coefficient of the structure

$\phi_s(f)$: phase lag due to wave reflection.

Provided that there is no wave damping or breaking along the wave flume, the transfer function T_k associated with any abscissa x_k is related to T_s by:

$$\begin{aligned} T_k &= T\ (x_k,f) = T_s.e^{i2\Theta_K} \\ \Theta_k &= m\ (x_k - x_s) \end{aligned} \tag{5}$$

The objective of the analysis is to estimate from records of water level variations three unknown functions of frequency: the incident wave power spectral density S_I, the reflection coefficient $C_R(f)$ and the phase lag $\phi_s(f)$ due to this reflection.

Let us now consider the relationship between the incident waves and the partially or totally standing waves observed in front of the structure. Since the observed water level variations are simply a linear superposition of the incident and reflected waves given by (1) and (3), the relationship between incident waves and observed waves is defined by the transfer function:

$$T_{\eta_K \eta_i} = 1 + T(x_k, t) \tag{6}$$

and the relationship between the spectrum of the observed waves $S_K(f)$ and the spectrum of the incident waves $S_I(f)$ is:

$$S_K(f) = S_I(f) \cdot T_{\eta_K \eta_i} \cdot T^*_{\eta_K \eta_i} \tag{7}$$

Where T^* stands for the complex conjugate of T.

From equations (4) to (7), the following expressions result:

$$S_K(f) = S_I(f) \cdot [1 + 2\mathrm{Re}(T_s) \cos 2\theta_K - 2\mathrm{Im}(T_s) \sin 2\theta_K + |T_s|^2] \tag{8}$$

$$S_K(f) = S_I(f) \cdot [1 + 2C_R(f) \cdot \cos(2\theta_K + \phi_s) + C_R^2(f)] \tag{9}$$

ANALYSIS WITH TWO WAVE GAUGES

From measurements of water level variations η_j, η_k at two locations x_j, x_k, it is possible to estimate the spectra $S_j(f)$ and $S_K(f)$, which are related to the unknown functions S_I, C_R and ϕ_s by equations similar to (8) and (9). It is also possible to obtain the cross-spectrum:

$$\begin{aligned} S_{jk}(f) &= C_{jk}(f) - i\, Q_{jk}(f) = \int_{-\infty}^{+\infty} R_{jk}(t)\, e^{-i2\pi ft} dt \\ R_{jk}(\tau) &= E\left[\eta(x_j, t) \cdot \eta(x_k, t - \tau)\right] \end{aligned} \tag{10}$$

The following relationship holds between the cross-spectrum $S_{jk}(f)$ and the incident wave spectrum $S_I(f)$:

$$\begin{aligned} S_{jk} &= S_I(f) T_{\eta_j \eta_i} \cdot T^*_{\eta_k \eta_i} \\ S_{jk} &= S_I(f) \cdot [1 + T_j] \cdot [1 + T_k^*] \\ S_{jk} &= S_I(f) \cdot [1 + T_s e^{i2\theta_j}] \cdot [1 + T_s^* e^{-i2\theta_k}] \end{aligned} \tag{11}$$

By separating the real and imaginary parts of (11), we obtain the co-spectrum and quad-spectrum:

$$\begin{aligned} C_{jk}(f) = S_I(f) \{ &[1 + |T_s|^2] \cdot \cos(\theta_j - \theta_k) + 2\,\mathrm{Re}(T_s) \cos(\theta_j + \theta_k) \\ &- 2\,\mathrm{Im}(T_s) \sin(\theta_j + \theta_k) \} \end{aligned} \tag{12}$$

$$Q_{jk}(f) = S_I(f)\ (1 - |T_s|^2).\ \sin(\theta_j - \theta_k) \tag{13}$$

For simplicity, we shall write hereafter:

$$\theta_{jk} = \theta_j - \theta_k = m\,(x_j - x_k) \tag{14}$$

With the expressions of $S_j(f)$, $S_k(f)$ given by (8) and the expressions of the co and quad-spectra given by (12) (13), we have a set of four linear equations with three unknown functions of frequency $Re(T_s)$, $Im(T_s)$ and $|T_s|^2$. A necessary and sufficient condition for having a non zero solution of this set of equations is:

$$\begin{vmatrix} 2\cos 2\theta_j & -2\sin 2\theta_j & 1 & S_j/S_I - 1 \\ 2\cos 2\theta_k & -2\sin 2\theta_k & 1 & S_k/S_I - 1 \\ 2\cos(\theta_j+\theta_k) & -2\sin(\theta_j+\theta_k) & \cos\theta_{jk} & C_{jk}/S_I - \cos\theta_{jk} \\ 0 & 0 & -\sin\theta_{jk} & Q_{jk}/S_I - \sin\theta_{jk} \end{vmatrix} = 0 \tag{15}$$

This condition gives the following expression of the incident wave spectrum:

$$S_{Ijk}(f) = \frac{S_j + S_k - 2\,(C_{jk}\cos\theta_{jk} - Q_{jk}\sin\theta_{jk})}{4\sin^2\theta_{jk}} \tag{16}$$

The subscript jk is added to indicate that this is an estimate of $S_I(f)$ derived from the wave records at abscissas x_j and x_k.

The spectra of the incident and reflected waves are related by:

$$S_R(f) = C_R^2(f).\ S_I(f) = |Ts|^2.\ S_I(f) \tag{17}$$

From (16) and (17) we get the following expression of the reflected wave spectrum:

$$S_{Rjk}(f) = \frac{S_j + S_k - 2\,(C_{jk}\cos\theta_{jk} + Q_{jk}\sin\theta_{jk})}{4\sin^2\theta_{jk}} \tag{18}$$

Expressions (16) and (18) are similar to those used by Kajima (3). Differences come only from the orientation of the positive x axis in opposite directions. From the preceding set of equations we can also derive the following expression for the transfer function:

$$T_{Sjk}(f) = \frac{-S_j e^{-2i\theta k} - S_k e^{-2i\theta j} + 2C_{jk}\, e^{-i(\theta j+\theta k)}}{4S_I(f).\sin^2\theta_{jk}} \tag{19}$$

which can also be written as:

$$T_{Sjk}(f) = \frac{-S_j e^{-2i\theta k} - S_k e^{-2i\theta j} + 2C_{jk} e^{-i(\theta_j+\theta_k)}}{S_j+S_k-2(C_{jk}\cos\theta_{jk} - Q_{jk}\sin\theta_{jk})} \qquad (20)$$

CRITICAL FREQUENCIES

Formula (9) shows that the power spectral density of the actually observed waves is a periodic function of space, for a given frequency, with a period equal to one half of the wave length associated with this frequency.

For a given pair of wave gauges, there is a discrete number of frequencies f_{cjk}, for which the distance between the wave gauges is a multiple of half the corresponding wave length $L(f_{cjk})$.

$$x_j - x_k = \pm p \frac{L}{2} (f_{cjk}) \qquad p = 1, 2, 3... \qquad (21)$$

For those critical frequencies, the following properties should hold:

$$\left.\begin{aligned} &S_j(f) = S_k(f) \\ &C_{jk}(f) = \pm S_k(f) \qquad C_{jk}\cos(\theta_j-\theta_k) > 0 \\ &Q_{jk}(f) = 0 \\ &\sin(\theta_j-\theta_K) = 0 \end{aligned}\right\} \; f = f_{cjk} \qquad (22)$$

As a result the numerator and denominator of (16) and (18) tend towards zero and the incident and reflected wave spectra cannot be evaluated with these formulae for these specific frequencies.

Because of round-off errors and background noise the numerator does not actually vanish, and it is observed in numerical computations that the absolute value of S_I and S_R increases considerably in the vicinity of the critical frequencies. This behaviour has been observed with all the methods of analysis based on measurements with two-gauge arrays.

Because of this difficulty, the distance between the wavegauges must be chosen carefully, with due consideration to the frequency range (fmin, fmax) over which the wave spectrum extends. Goda and Suzuki [2] suggest the following rule for this choice.

$$x_j - x_k = 0.05\, L(fmin) = 0.45\, L(fmax) \qquad (23)$$

ANALYSIS WITH THREE WAVE GAUGES

From simultaneous measurements of water level variations with a three-gauge array, nine functions of frequency are derived i.e. the three spectra S_1, S_2, S_3 corresponding to the observed partially standing waves at the gauge locations, the three co-spectra C_{21}, C_{31}, C_{32} and quad-spectra Q_{21}, Q_{31}, Q_{32} associated with the different couples of gauges.

With each of these functions, is associated an equation such as (8), (12) or (13). We thus have a set of nine equations for three unknown functions only. Since there are more data available than unknown parameters many different formulae can be derived for evaluating the incident wave spectrum and the transfer function representing the wave reflection from the structure. Many of these formulae are inappropriate because they cannot be applied for critical frequencies associated with some or all of the gauge intervals.

A theoretical analysis developed in [1] led us to the following formulae for evaluating the incident and reflected wave spectra:

$$\begin{aligned} S_I(f) &= \alpha_{21} S_{I21}(f) + \alpha_{31} S_{I31}(f) + \alpha_{32} S_{I32}(f) \\ S_R(f) &= \alpha_{21} S_{R21}(f) + \alpha_{31} S_{R31}(f) + \alpha_{32} S_{R32}(f) \end{aligned} \tag{24}$$

$$\alpha_{21} + \alpha_{31} + \alpha_{32} = 1 \qquad \alpha_{jk} \geq 0 \tag{25}$$

S_{Ijk} and S_{Rjk} are estimates of the incident and reflected wave spectra obtained from (16) and (18) for the different possible associations of gauges by pairs.

The weighting factors α_{jk} are positive functions of frequency, defined in such a way that (24) be valid for all frequencies, of interest, including for the critical values associated with the different gauge intervals. For this to be true, the gauge locations must be chosen so as to avoid any coincidence of the critical frequencies associated with the different gauge spacings; otherwise, effects similar to those observed with a two-gauge array would be encountered for these frequencies.

For critical frequencies f_{c12}, S_{I12} cannot be computed from (16) as shown in the preceding section, so α_{21} should vanish for this frequency. By an analysis of equations (8), (12), (13), it can be shown that solutions given by (16) for S_{I32}, S_{I31} and by (18) for S_{R32}, S_{R31} are theoretically equivalent for these critical frequencies. However, since slight differences may result from background noise $S_I(f)$ and $S_R(f)$ are estimated by:

$$S_I(f_{C12}) = 0.5\ (S_{I31} + S_{I32})$$
$$S_R(f_{C12}) = 0.5\ (S_{R31} + S_{R32}) \tag{26}$$

Similar formulae are used for the critical frequencies f_{C31}, f_{C32} associated with the other gauge intervals. The weighting functions are thus subject to the conditions:

$$\begin{aligned} &\alpha_{jk}(f) \to 0 \\ &\alpha_{j1}(f) \to 1/2 \qquad \text{for} \quad f \to f_{cjk} \\ &\alpha_{k1}(f) \to 1/2 \end{aligned} \tag{27}$$

We use the following functions, which satisfy conditions (25) and (27):

$$\alpha_{jk}(f) = \frac{\sin^{2n}\theta_{jk}}{S_\alpha^{(n)}} \qquad n = 1, 2, 3\ldots$$
$$S_\alpha^{(n)} = \sin^{2n}\theta_{21} + \sin^{2n}\theta_{31} + \sin^{2n}\theta_{32} \tag{28}$$

Insertion of these functions in (24), for n = 1 and 2, leads to:

$$\begin{matrix} S_I(f) \\ S_R(f) \end{matrix} = \frac{\overline{S}^{(n)} - \overline{C}^{(n)} \pm \overline{Q}^{(n)}}{2\ S_\alpha^{(n)}} \tag{29}$$

$$\begin{aligned} \overline{S}^{(1)} &= S_1 + S_2 + S_3 \\ \overline{C}^{(1)} &= C_{21}\cos\theta_{21} + C_{31}\cos\theta_{31} + C_{32}\cos\theta_{32} \\ \overline{Q}^{(1)} &= Q_{21}\sin\theta_{21} + Q_{31}\sin\theta_{31} + Q_{32}\sin\theta_{32} \end{aligned} \tag{30}$$

$$\begin{aligned} \overline{S}^{(2)} &= 0.5(S_1+S_2)\sin^2\theta_{21} + 0.5(S_1+S_3)\sin^2\theta_{31} + 0.5(S_2+S_3)\sin^2\theta_{32} \\ \overline{C}^{(2)} &= C_{21}\cos\theta_{21}\sin^2\theta_{21} + C_{31}\cos\theta_{31}\sin^2\theta_{31} + C_{32}\cos\theta_{32}\sin^2\theta_{32} \\ \overline{Q}^{(2)} &= Q_{21}\sin^3\theta_{21} + Q_{31}\sin^3\theta_{31} + Q_{32}\sin^3\theta_{32} \end{aligned} \tag{31}$$

The transfer function associated with the wave reflection on the coastal structure is estimated by means of:

$$T_S(f) = \frac{N_{21}\sin^2\theta_{21} + N_{31}\sin^2\theta_{31} + N_{32}\sin^2\theta_{32}}{D_{21}\sin^2\theta_{21} + D_{31}\sin^2\theta_{31} + D_{32}\sin^2\theta_{32}} \tag{32}$$

with:

$$\begin{aligned} N_{jk} &= -S_j\, e^{-i2\theta_k} - S_k\, e^{-i2\theta_j} + 2\, C_{jk}\, e^{-i(\theta_j+\theta_k)} \\ D_{jk} &= S_j + S_k - 2\,(C_{jk}\cos\theta_{jk} - Q_{jk}\sin\theta_{jk}) \end{aligned} \tag{33}$$

N_{jk} and D_{jk} are the terms involved in (20) when estimating the transfer function from each pair of gauges.

The reflection coefficient of the structure can be estimated by two possible methods:

- the first is by the use of (17) with the expressions of S_I and S_R given by (24), i.e. by (29) (30) (31) for the two lowest orders of the weighting functions.
- the second is by the use of (4) with the transfer function given by (32) and (33).

In the following we refer to these two estimates as $C_R(f)$ and $C'_R(f)$ respectively.

APPLICATION TO LABORATORY EXPERIMENTS

Examples of application of the present method to random-wave experiments conducted at Sogreah's laboratory will now be given.

EXPERIMENTAL SET-UP

The experiments were performed in a wave tank of 39 m length, 1.40 m depth and 0.60 m width, with the set-up indicated in figure 1. The bottom profile conforms to an actual situation for which breakwater stability tests were required. Two kinds of structures were considered at a scale of 1/50:

a) a rubble mound breakwater with a two layer tetrapod covering on a seaward slope of 4/3.

b) a vertical sea-wall with an anti-reflection chamber (ARC system), as described in [6]

Though a three-gauge array is generally sufficient for applying the present method, a four-gauge array was used in these particular experiments, in order to compare the results provided by the four different combinations of gauges by triplets. Water level variations were measured with capacitance-type wave gauges.

Figure 1 shows one of the wave-gauge arrangements used. In this case, gauges 1 and 4 are located respectively at the third anti-node and third node of the partially standing waves corresponding to the spectral peak frequency.

Data retrieval and digitization of water level measurements were performed on a General Automation GA220 minicomputer of 16 Kwords capacity. A Fortran computer code based on the previously described method, is implemented on this computer for current experiments.

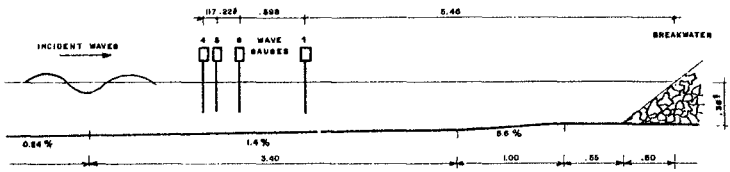

Fig.1 EXPERIMENTAL SET-UP

Model 1 - BREAKWATER WITH TETRAPODS

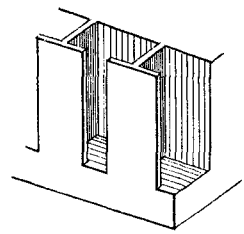

Model 2 : SEA-WALL WITH ARC SYSTEM

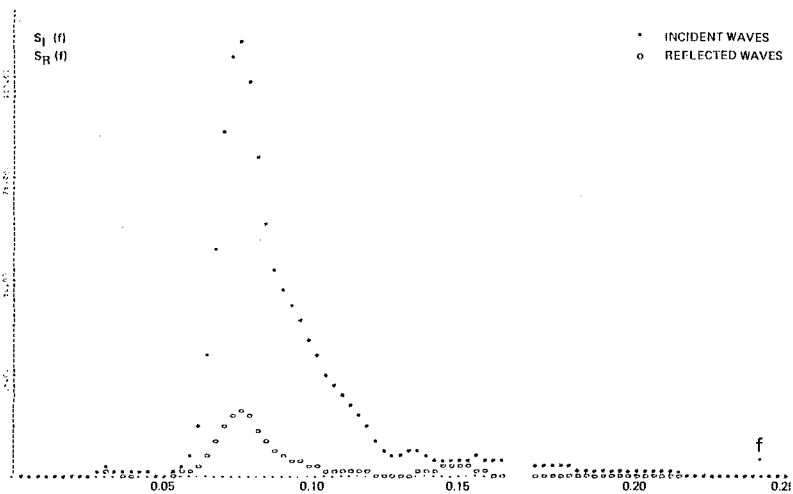

Fig. 2 Incident and reflected wave spectra obtained with model 1

For processing the data of the four-gauge array and for comparing the results of the four different triplets, a special code was implemented on an ITEL AS 6 computer.

Wave records were analysed over a period of 160 s, with a time step of 0.1 s. Auto and cross-covariance functions were computed with a maximum lag of $\pm$ 10 s. This analysis provided values of the 16 following functions with a frequency interval of 0.02 Hz at model scale, i.e. of 0.0028 Hz at prototype scale:

- the spectra of waves observed at the gauge locations S_1, S_2, S_3, S_4
- the six co-spectra C_{21}, C_{31}, C_{41}, C_{32}, C_{42}, C_{43}
- the six quad-spectra Q_{21}, Q_{32}, Q_{41}, Q_{32}, Q_{42}, Q_{43}

The number of degrees of freedom associated with the preceding parameters is approximately 40, with a Hamming spectral window. From the Chi-square law it is concluded that the 80% confidence interval lies between 73% and 130% of the estimated power spectral density.

INCIDENT AND REFLECTED WAVE SPECTRA

Figure 2 shows the incident and reflected wave spectra derived from the wave records of gauges 2, 3, 4 of figure 1, with the first type of structure, by application of formulae (29) and (31).

Figure 3 gives a simultaneous plot of the incident wave spectra obtained by analysis of the four different combinations of wave gauges (O stands for gauges 1, 2, 3; v for gauges 1, 2, 4; x for gauges 1, 3, 4 and * for gauges 2, 3, 4). As this graph results from a printer output, coincident values of the power spectral densities are plotted by a single symbol. The four estimates of the incident wave spectrum are in excellent agreement.

Figure 4 gives a simultaneous plot of the incident wave spectra obtained by analysis of the four gauges with the two lowest orders of weigthing functions (28) (* stands for n=1 and O for n=2). No significant difference appears here between the two procedures of estimation of the incident wave spectrum.

The same conclusions were drawn from tests with the second type of structure.

With this technique, the gauge locations should be chosen so as to avoid too proximate values of the critical frequencies associated with the different intervals. Figure 5 refers to a particular wave gauge arrangement, 1, 2, 4, where critical frequencies associated with the gauge intervals are very nearly coincident, so that $S_{\alpha}^{(n)}$, defined by (28), drops to a very low value for frequencies near f=1.55 Hz at model scale and f=0.22 Hz at prototype scale. This situation leads to undesirable effects shown in figures 6 and 7.

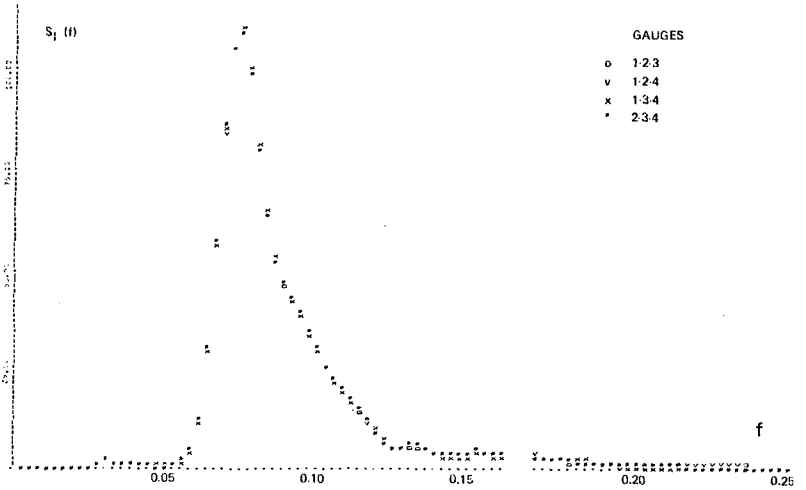

Fig. 3 Incident wave spectrum resulting from 4 different 3 - gauge arrays with n = 2

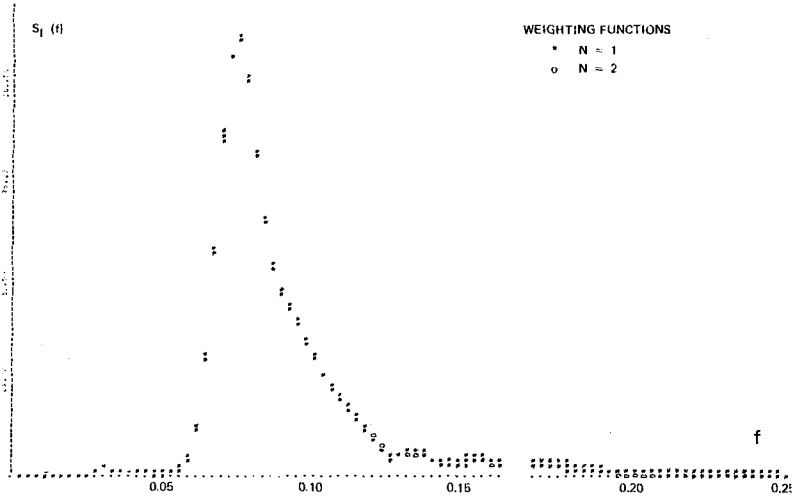

Fig. 4 Incident wave spectrum obtained with weighting functions of order n = 1 & 2

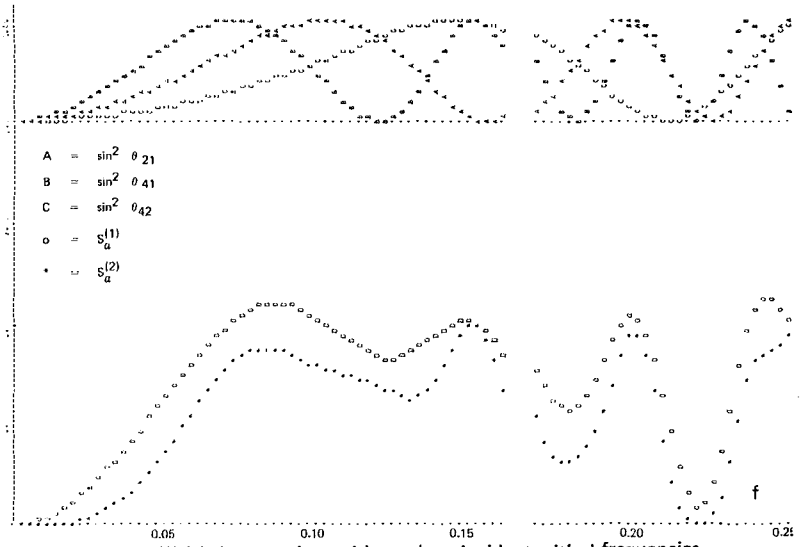

Fig. 5 Weighting functions with nearly coincident critical frequencies

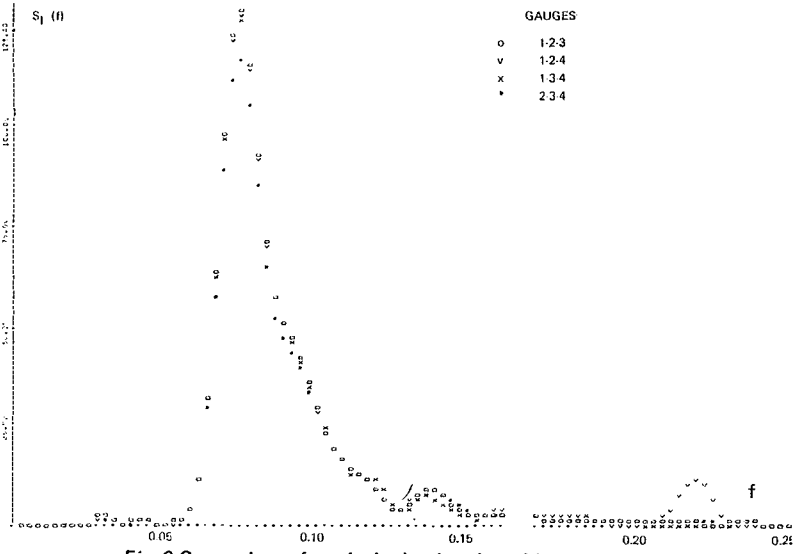

Fig. 6 Comparison of results in the situation of Fig. 5, for gauges 1-2-4

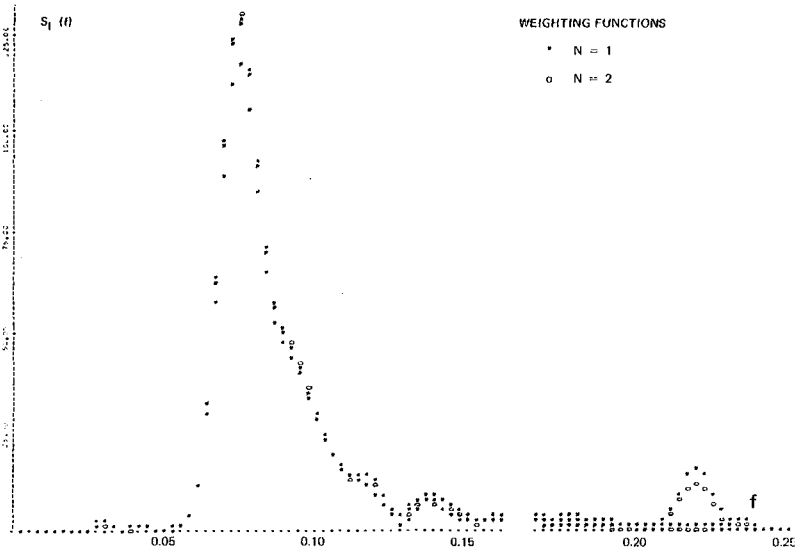

Fig. 7 Effect of weighting parameter n in the situation of fig. 5

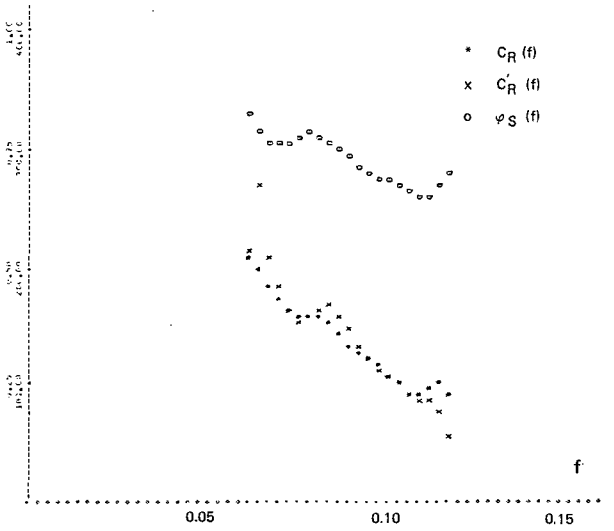

Fig. 8 Reflection coefficients and phase lag for model 1

In figure 6, it is seen that the incident wave spectrum estimated from gauges 1, 2, 4 exhibits a small hump in the vicinity of the previously mentioned frequency, while this is not observed with the spectra estimated from the three other gauge associations.

Figure 7 is a graph similar to figure 4. It shows that the weighting functions of order 1 gives a hump of greater magnitude than those of order 2, in the frequency interval where critical frequencies are nearly coincident, while results are almost the same for other frequencies. Because of this, preference should be given to (31) for evaluating the incident and reflected wave spectra.

Another point should be stressed about the presentation of wave spectra derived through this analysis. The frequency $f=0$ is a critical frequency whatever the choice of the gauge intervals, since $\sin \theta_{jk}$ vanishes for this value. For this reason, a sharp rise in the absolute value of $S_I(f)$ and $S_R(f)$ is observed at very low frequencies, with a three-gauge array as well as with a two-gauge array. This effect was illustrated in [1] with numerically simulated random waves, for which it was clear that no energy was actually present in the low frequency range. This spurious effect affects a frequency interval equal to the width of the specific spectral window used for smoothing wave spectra. A cut-off frequency equal to this bandwidth is introduced in the computations.

REFLECTION COEFFICIENTS

Figures 8 and 9 show the variation with frequency of the reflection coefficients $C_R(f)$, $C'_R(f)$ for the two structures previously mentioned, together with the phase lag $\phi_s(f).C_R(f)$ is derived here by means of the weighting functions of order 2.

It was shown in [1], with numerically simulated water waves, that a good estimate of the reflection coefficients cannot be obtained for frequencies where the power spectral density is very low. A threshold value dependent on the peak spectral density, was accordingly chosen for selecting the frequency range over which these parameters are computed. Results are presented here for a threshold value of 10%.

The two procedures described for evaluating the reflection coefficient of the structure versus frequency, though theoretically equivalent, give slightly different estimates of this parameter. Both procedures give the same general trend which is typical of the structures considered. The rubble-mound breakwater exhibits a progressive decrease in reflection as frequency increases, due to higher dissipation as waves impinge on the artificial blocks. The ARC system on the other hand exhibits a U-shaped curve, with minimum reflection for a frequency dependent on the dimensions of the anti-reflection chamber, which acts as a resonator.

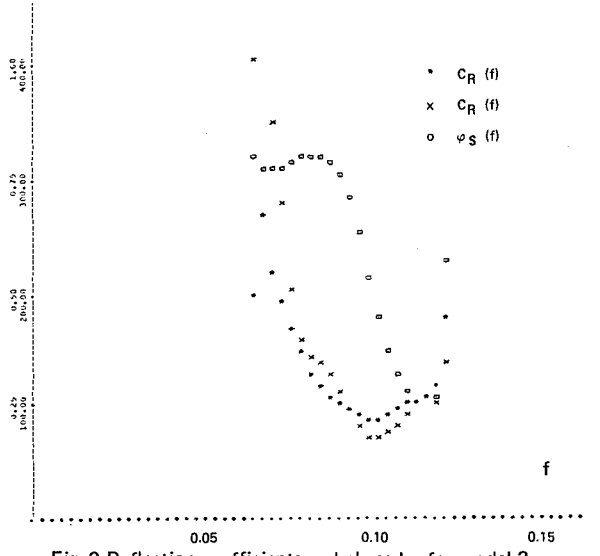

Fig. 9 Reflection coefficients and phase lag for model 2

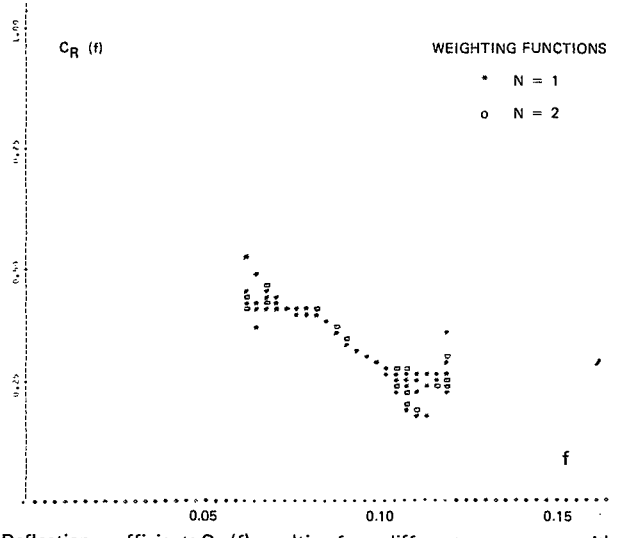

Fig. 10 Reflection coefficients $C_R(f)$ resulting from different gauge arrays with n = 1 & 2

As shown on figures 8 and 9 $C_R(f)$ has generally a more regular variation as a function of frequency than $C'_R(f)$. The reason for this behaviour has not yet been fully understood. From our experiments, the differences between $C_R(f)$ and $C'_R(f)$, did not seem to be connected with non-linear effects, as they did not increase with the significant wave height of the waves considered.

Figure 10 compares the reflection coefficients $C_R(f)$, associated with the first and second order weighting functions (28): * stands for n=1, 0 for n=2. As this graph results from a printer output, coincident values of $C_R(f)$ by both methods are plotted by a single symbol. Results shown here come from the analysis of the four combinations of gauges. A generally good agreement is observed between results of different triplets, and between the two methods of estimations of $C_R(f)$ for frequencies where wave energy is high. The scatter of experimental points increases on the boundaries of the wave spectrum.

CONCLUSION

In conclusion, the method of analysis just described has proven to be a valuable tool for estimating incident and reflected wave spectra in instances where wave reflection on structures has to be accounted for. Examples of application of the method to flume experiments have been given here. The method should also be applicable to field investigations, provided that the incoming waves are directed normally to the reflecting structure.

The numerical and experimental tests have shown that the incident wave spectrum is estimated accurately, provided that the gauge spacings are properly selected, so as to avoid too small a frequency interval between critical frequencies. The incident wave spectrum is practically insensitive to the order of the weighting functions used, except when critical frequencies are nearly coincident.

The method also proves to be an interesting means of studying the reflection coefficient (and the associated phase lag) of coastal structures as a function of frequency. It enables a better assessment of the efficiency of wave absorbing devices, such as the ARC system.

Two procedures of evaluation of the reflection coefficient have been investigated, one directly connected with the incident and reflected wave spectral densities by equations (17) and (29), the other derived from the theoretical transfer function (32). The first one is considered preferable since it showed a more regular variation of the reflection coefficient versus frequency.

REFERENCES

(1) P. Gaillard
Méthode d'analyse de la houle irrégulière produite en canal en présence d'un ouvrage réfléchissant - SOGREAH, NT 1834, Décembre 1976

(2) Y. Goda & Y. Suzuki
Estimation of incident and reflected waves in random wave experiments. Proc. 15th Coastal Eng. Conf. Honolulu, Hawaii, July 1976, p. 828-845

(3) R. Kajima
Estimation of an incident wave spectrum under the influence of reflection - Proc. 13th Congress of IAHR, Kyoto Japan 1969, Vol. 5.1 (Seminars), p. 285-288

(4) D.B. Morden, E.P. Richey & D.R. Christensen
Decomposition of coexisting random wave energy. Proc. 15th Coastal Eng. Conf. Honolulu, Hawaii, July 1976, p. 846-865

(5) E.B. Thornton & R.J. Calhoun
Spectral resolution of breakwater reflected waves. J. Waterways, harbors and coastal Eng. Proc. ASCE WW4 November 1972, p. 443-460

(6) L. Tourmen, J.P. Montaz, L. Doublet
Un nouveau dispositif amortissant la reflexion des vagues sur les parois verticales : la chambre anti-reflexion (ARC), 17e Congrès AIRH Baden-Baden, RFA, août 1977, Sujet C6, p. 41-48.